



## DIAMOND-LIKE CARBON TARGETS FOR EXTREME-INTENSITY LASER–MATTER INTERACTION

Cosmin JALBĂ, Nikolay DJOURELOV

Extreme Light Infrastructure-Nuclear Physics, “Horia Hulubei” National R&D Institute for Physics and Nuclear Engineering,  
077125 Magurele, Romania

Corresponding author: Cosmin JALBĂ, E-mail: [cosmin.jalba@eli-np.ro](mailto:cosmin.jalba@eli-np.ro)

**Abstract.** Diamond-like carbon (DLC) thin films have emerged as highly reliable ultra-thin targets for relativistic laser–matter interaction studies owing to their exceptional mechanical resilience, high  $sp^3$  bonding fraction, and low impurity content. These properties allow DLC membranes only tens of nanometers thick to maintain structural integrity under the extreme thermal and mechanical conditions imposed by high-intensity, ultrashort laser pulses. In this work, we investigate free-standing DLC films fabricated by plasma-enhanced chemical vapor deposition (PECVD) and released through a controlled copper back-etching process. The structural, chemical, and morphological characteristics of the films are examined using X-ray photoelectron spectroscopy (XPS) and optical microscopy. Analysis of  $sp^2/sp^3$  hybridisation, surface oxygen functionality, and membrane uniformity demonstrates that the films meet the stringent requirements of petawatt-class laser facilities. These results confirm that PECVD-grown free-standing DLC membranes provide robust, reproducible, and high-quality targets suitable for advanced ion-acceleration regimes including TNSA, RPA, BOA, and relativistic transparency.

**Keywords:** diamond-like carbon, ultra-thin films, relativistic laser-matter-interaction,  $sp^2/sp^3$  hybridization, free-standing membranes, ion acceleration.

### 1. INTRODUCTION

Diamond-like carbon (DLC) ultra-thin foils have emerged as some of the most robust and reliable target materials for high-intensity laser–matter interaction experiments, owing to their unique combination of exceptional mechanical strength, high  $sp^3$  hybridisation, low intrinsic impurity levels, and the ability to reproducibly control thickness down to the few-nanometre regime. These attributes give DLC membranes a decisive advantage over polymeric or metallic foils, which often suffer from premature deformation, melting, or structural failure under the extreme thermodynamic conditions characteristic of petawatt (PW) laser systems. At intensities approaching or exceeding  $10^{21}$  W/cm<sup>2</sup>, where sub-30 fs pulses interact with ultra-thin foils on femtosecond timescales, the leading edge of the pulse can induce rapid pre-expansion and pre-plasma formation in conventional materials, severely compromising the ensuing acceleration dynamics. In contrast, hydrogenated DLC films with high  $sp^3$  content exhibit exceptional resilience to ultrafast heating, maintaining structural integrity during the rising edge of high-contrast pulses and thereby supporting the stringent requirements of advanced relativistic acceleration regimes [8, 9].

This intrinsic robustness has made DLC foils a versatile platform for a broad range of ion-acceleration mechanisms. Their stability under intense irradiation enables reliable operation in target-normal-sheath acceleration (TNSA), radiation-pressure acceleration (RPA), breakout afterburner (BOA), and transparency-driven acceleration, where maintaining uniformity, suppressing contamination, and tightly controlling target areal density are critical [2–5, 15]. As a result, DLC targets have been adopted across major PW laser facilities and have demonstrated consistent performance across diverse experimental geometries, highlighting their importance as a foundational platform for next-generation relativistic plasma physics.

A key limitation of ultra-thin targets lies in their susceptibility to pre-pulse effects. Even in advanced PW systems employing plasma mirrors, cross-polarised wave (XPW) generation, or OPCPA architectures, temporal contrast remains finite, with pre-pulse intensities commonly in the  $10^9$ – $10^{11}$  W/cm<sup>2</sup> range [16, 17].

CH-polymer foils, widely used in earlier studies, undergo rapid thermal softening, rarefaction, and partial ablation at these levels, long before the arrival of the main pulse. Such pre-expansion disrupts density profiles required for RPA, shifts transparency thresholds, and suppresses electron reflux essential for strong TNSA sheaths. By contrast, the cross-linked  $sp^3$ -rich structure of hydrogenated DLC provides far superior resistance to sub-ablative heating, ensuring that the foil remains near solid density throughout the pre-pulse window [8,9]. This superior resilience explains the transition toward DLC membranes in modern relativistic-plasma experiments.

Equally essential is the requirement that these films be truly free-standing. Supported ultra thin foils experience hydrodynamic and thermal disturbances transmitted from their substrates, including shock fronts, thermal waves, and parasitic plasma plumes that compromise interaction reproducibility [9, 16]. Substrates also inhibit electron reflux – multiple recirculation cycles of hot electrons that critically enhance sheath formation in TNSA and influence ion-energy scaling. Free-standing DLC membranes eliminate these complications entirely, ensuring pristine density gradients, unimpeded electron recirculation, and a contamination-free interaction volume. This becomes especially critical in PW facilities operating with tight-focus optics ( $f/1$ – $f/3$ ), where even micron-scale support structures distort the focal spot or generate unwanted plasma.

Numerous studies have demonstrated the performance of DLC targets across relativistic regimes. Steinke *et al.* reported efficient carbon-ion acceleration from few-nanometre DLC membranes during relativistic transparency [18]. Henig *et al.* demonstrated phase-stable RPA using circularly polarised pulses interacting with nanometre-scale DLC foils [5]. At LMU Munich, DLC combined with CNT foams enhanced pulse steepening and self-focusing, yielding higher-energy carbon ions [19]. Earlier work by Liechtenstein *et al.* established DLC as a reliable material for self-supported ultra-thin accelerator targets [20], while more recent high-repetition-rate platforms leveraged DLC's reproducibility for consistent TNSA performance [12]. Additional experiments confirmed DLC's suitability for relativistic-transparency regimes, producing narrow-band ion bunches [4], multi-MeV carbon ions [2], and superponderomotive electrons relevant for multi-PW facilities [15].

At ELI-NP, the development of free-standing DLC targets fabricated by plasma-enhanced chemical vapour deposition (PECVD) followed by copper back-etching has become central to PW-class target production. Dincă *et al.* demonstrated a reproducible PECVD process for generating 50–180 nm free-standing membranes across millimetre-scale apertures, optimised specifically for PW interaction geometries [1]. These PECVD-grown ta-C:H films, characterised by high  $sp^3$  content and excellent uniformity, have already supported several experimental campaigns, demonstrating both mechanical stability under irradiation and reliable microstructural quality [10, 11].

While PECVD remains a highly effective method for producing hydrogenated, high- $sp^3$  DLC films, a key objective of ongoing work is to broaden the accessible fabrication parameter space. A promising direction involves magnetron-sputtered DLC deposited onto dissolvable NaCl sacrificial layers, which, once removed, yield contamination-free free-standing foils. Magnetron sputtering enables lower intrinsic stress, improved large-area uniformity, tunable bonding configuration, and the possibility of producing non-hydrogenated, high-density tetrahedral carbon films. These sputtered membranes will complement PECVD-grown targets, allowing systematic studies of ultra-thin-foil behaviour across TNSA, RPA, BOA, and transparency regimes, while providing researchers with a broader and more versatile suite of free-standing DLC target properties for next-generation PW laser systems.

## 2. EXPERIMENTAL METHODS

DLC films were first deposited directly onto polished copper substrates using the plasma-enhanced chemical vapor deposition (PECVD) procedure described in [1]. Prior to deposition, the copper substrates were prepared using a multilayer polishing protocol designed to produce a mirror-quality surface suitable for uniform thin-film growth. Following substrate cleaning and dehydration, PECVD was carried out at a pressure of approximately  $10^{-3}$  mbar using hydrocarbon precursors activated by a 13.56 MHz, 100 W RF discharge, consistent with established protocols for growing hydrogenated tetrahedral amorphous carbon (ta-C:H) [8]. Film thicknesses obtained under these conditions ranged from 53.6 nm to 178 nm.

After PECVD deposition, the DLC-coated copper substrates underwent the photolithographic back-etching sequence described in [1] to release the films as free-standing membranes. In this process, the photoresist was applied by spray coating, ensuring a uniform layer across the DLC surface without imposing shear forces that could damage the thin films. The coated substrates were then exposed through a UV mask, developed in NaOH solution, and subsequently subjected to copper dissolution in  $\text{FeCl}_3$ . Such back-etching techniques are widely used for fabricating ultra-thin self-supported foils for PW-class laser experiments, as they preserve the structural continuity and thickness uniformity of the deposited films [9–11]. The etching process produced circular apertures of approximately 1 mm diameter, across which the DLC films remained suspended as intact, free-standing membranes.

Only after the membranes were completely released from the copper substrate were they carefully transferred and affixed to custom 3D-printed supports. These supports were designed to provide mechanical stability and compatibility with high-power laser target-delivery systems while minimising contact with the free-standing region. The DLC films were secured to the frames using a controlled micro-adhesion process, ensuring firm attachment without introducing mechanical stress, deformation, or contamination that could compromise the integrity of the ultra-thin free-standing membranes. (See Figures 6, (a), (b), (c))

X-ray photoelectron spectroscopy (XPS) measurements were carried out after mounting, using a Mg  $K_\alpha$  radiation source and following established protocols for diamond-like carbon analysis. Prior to spectral acquisition, the samples were gently heated to remove physisorbed contaminants. High-resolution C 1s spectra were deconvolve into  $sp^2$ ,  $sp^3$ , C–O–C, C–O=C, and C=O–OH contributions using standard fitting models for amorphous carbon films [8].

## 2. RESULTS AND DISCUSSION

Survey XPS spectra confirm that carbon is the predominant elemental constituent of all samples, with only minor oxygen contamination and trace-metal residues, the latter likely introduced during the wet-etching process. Quantitative analysis indicates that these oxygen functionalities are confined to the uppermost nanometres of the films, consistent with prior observations for PECVD-grown ta-C:H [8, 9]. This surface oxidation does not significantly perturb the underlying bulk structure, preserving the intrinsic tetrahedral hybridisation network and ensuring that the mechanical and optical properties are dominated by the  $sp^3$ -rich carbon matrix rather than surface contaminants.

High-resolution C 1s spectra (Table 1) allow deconvolution of the  $sp^3$ ,  $sp^2$ , and C–O bonding contributions, revealing  $sp^3$  fractions ranging from 51.8% to 70.7%. These values are in excellent agreement with canonical PECVD ta-C:H growth behaviour, where ion-assisted deposition under energetic plasma conditions promotes tetrahedral coordination [8, 9]. Such  $sp^3$  fractions correspond to hydrogenated tetrahedral amorphous carbon structures with high cross-link densities, and they align closely with previously characterised  $sp^3$ -rich DLC materials used as targets in petawatt-class laser experiments [1, 5, 15]. These hybridisation ratios are directly correlated with mechanical stiffness, intrinsic compressive stress, and the ability of the film to withstand ultrafast laser irradiation without significant pre-expansion or ablation.

Table 1

XPS data on hybridization ratios determined in the C 1s peak for DLC films

XPS analyzed sample	Sample signal of + Traces of	C 1s - $sp^2/sp^3$ ratio	$sp^3$ (%)
DLC (178 nm)	Cu + Fe, Cl, Ni	$0,22 \pm 0,02$	(70,4 ± 3,5)
DLC (163 nm)	Cu + Fe, N	$0.36 \pm 0.02$	(70,7 ± 3,5)
DLC (120 nm)	Cu + Fe	$0.81 \pm 0.11$	(51,8 ± 2,6)
DLC (100 nm)	Cu + Fe, Na	$0.27 \pm 0.02$	(65,1 ± 3,26)
DLC (53,6 nm)	Cu + Fe, Na, N	$0.16 \pm 0.01$	(70,4 ± 3,5)

The 178 nm and 163 nm films (Figs. 1a and 2a) display the highest  $sp^3$  fractions (70.4% and 70.7%), consistent with earlier reports that thicker PECVD layers favour tetrahedral bonding due to the stabilising effect of prolonged energetic ion bombardment. The resulting dense tetrahedral networks generate strong intrinsic compressive stresses and enhance thermal stability, both critical for maintaining solid-density conditions during the interaction with ultrahigh-intensity laser pulses [10, 15].

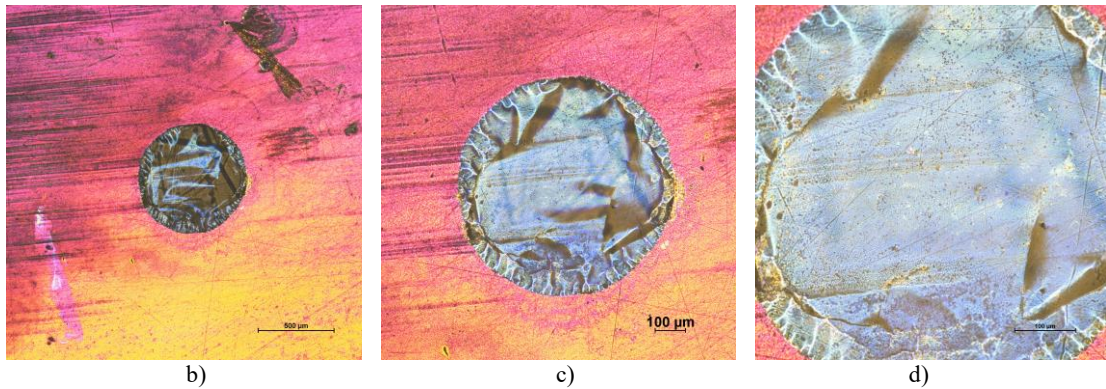
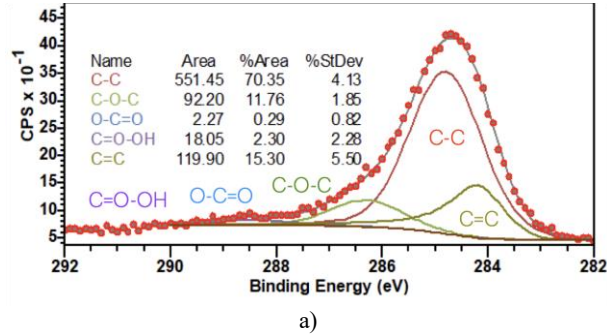


Fig. 1 - a) C 1s spectra for 178 nm DLC free-standing film and Optical Microscopy – (b), (c), (d).

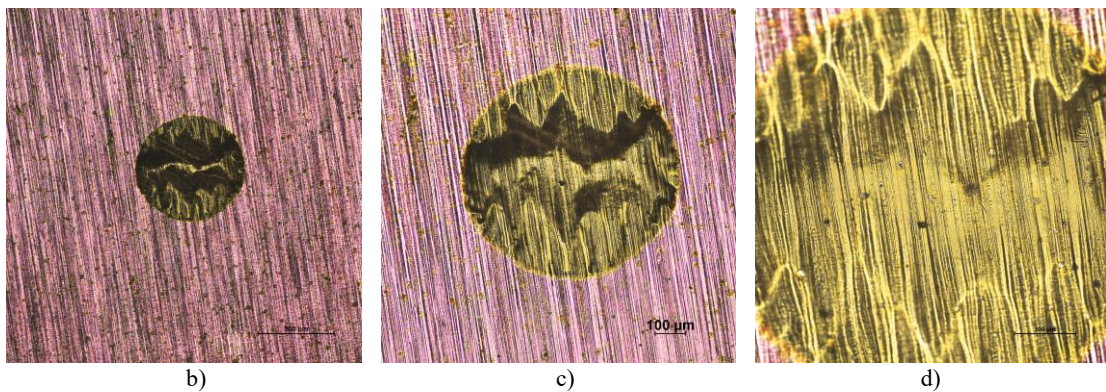
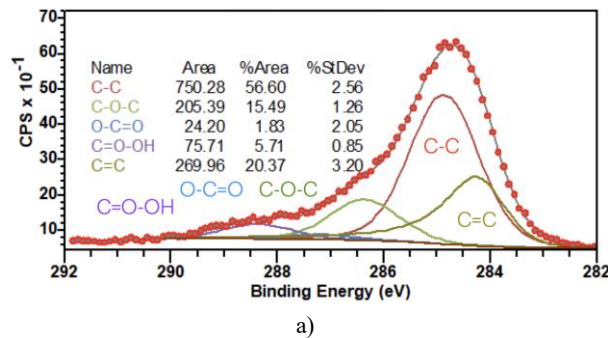
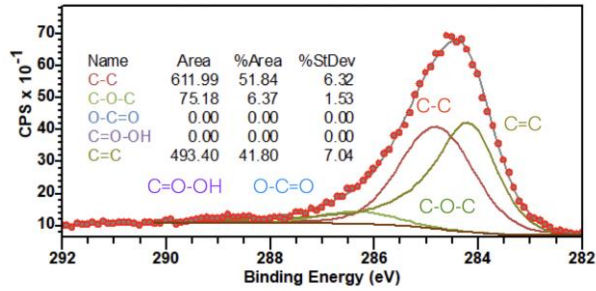


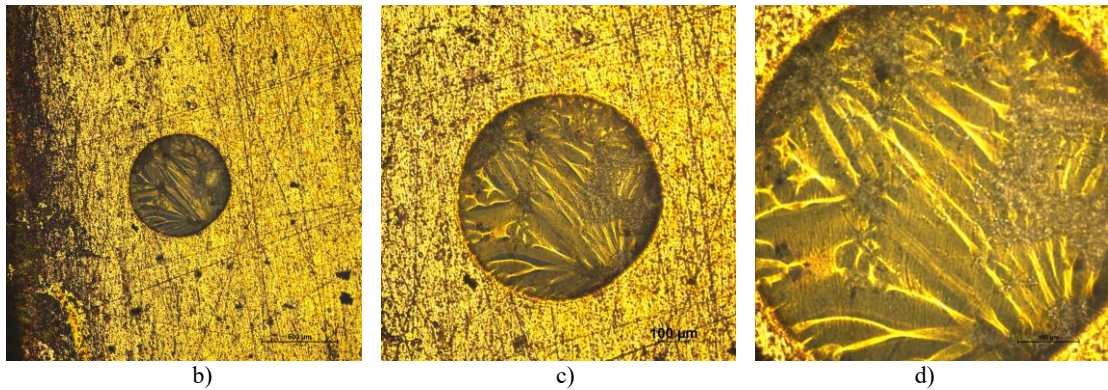
Fig. 2 - a) C 1s spectra for 163 nm DLC free-standing film and Optical Microscopy – (b), (c), (d).

The  $sp^3$  content in these films is approximately 36% higher than in the thinnest 120 nm film, supporting minimal pre-expansion, which is essential for optimal radiation pressure acceleration (RPA) and relativistic transparency regimes (Fig. 3a).

Conversely, the 120 nm film exhibits the lowest  $sp^3$  fraction (51.8%), reflecting the typical reduction in tetrahedral bonding and concurrent increase in  $sp^2$  clustering observed in lower-density PECVD DLC films [8]. The increased  $sp^2$  content and reduced cross-link density correlate with lower mechanical stiffness, higher thermal conductivity, and enhanced susceptibility to pre-pulse heating, which may compromise structural integrity under ultrafast irradiation. The 100 nm film (65.1%  $sp^3$ ) demonstrates intermediate mechanical and thermal behaviour, consistent with previous reports indicating that mid-range  $sp^3$  fractions offer an optimal balance of rigidity and flexibility for high-repetition laser operation in the TNSA regime (Fig. 4a) [11].



a)



b)

c)

d)

Fig. 3 – a) C 1s spectra for 120 nm DLC free-standing film and Optical Microscopy – (b), (c), (d).

Interestingly, the 53.6 nm film (Fig. 5a) achieves a high  $sp^3$  fraction of 70.4%, comparable to the thickest samples. This can be attributed to enhanced tetrahedral incorporation during the early stages of PECVD growth, where energetic subsurface ion bombardment preferentially stabilises  $sp^3$  bonding, even in ultra thin layers [8]. This results in a highly cross-linked, mechanically stiff network despite minimal thickness. The high  $sp^3$  content minimizes the absorption of background illumination and ensures reliable performance in transparency-driven acceleration, corroborating prior findings from studies on ultra-thin DLC membranes under relativistic transparency conditions [15, 17].

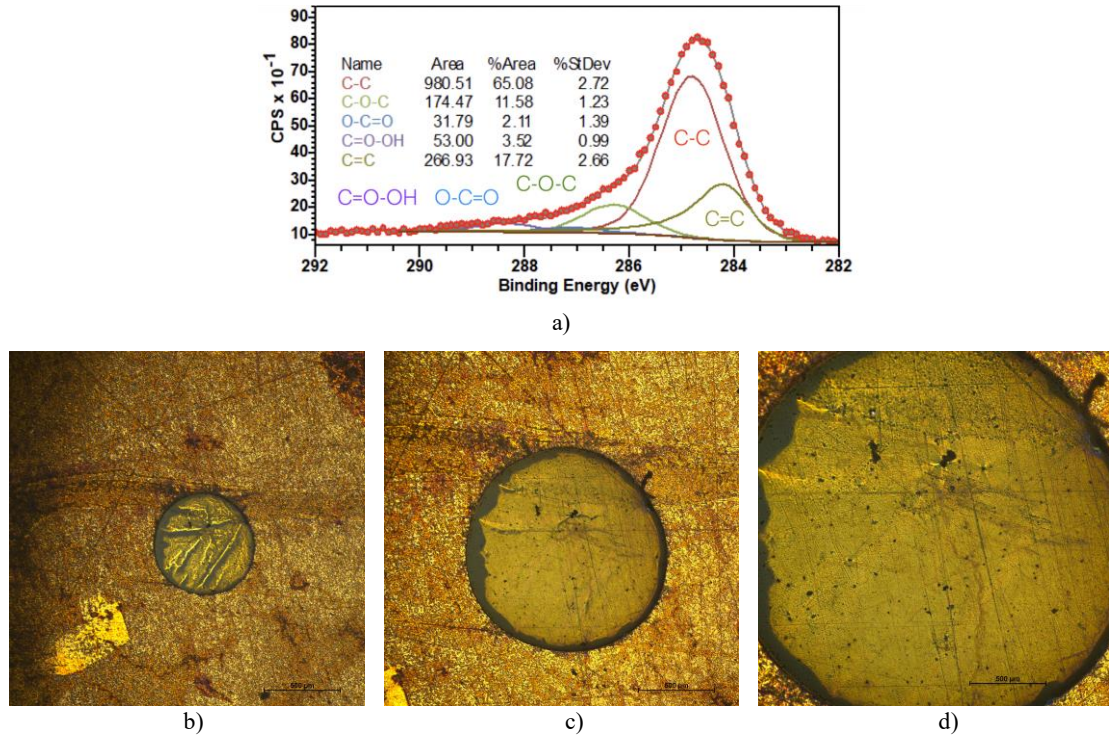


Fig. 4 – a) C 1s spectra for 100 nm DLC free-standing film and Optical Microscopy – (b), (c), (d).

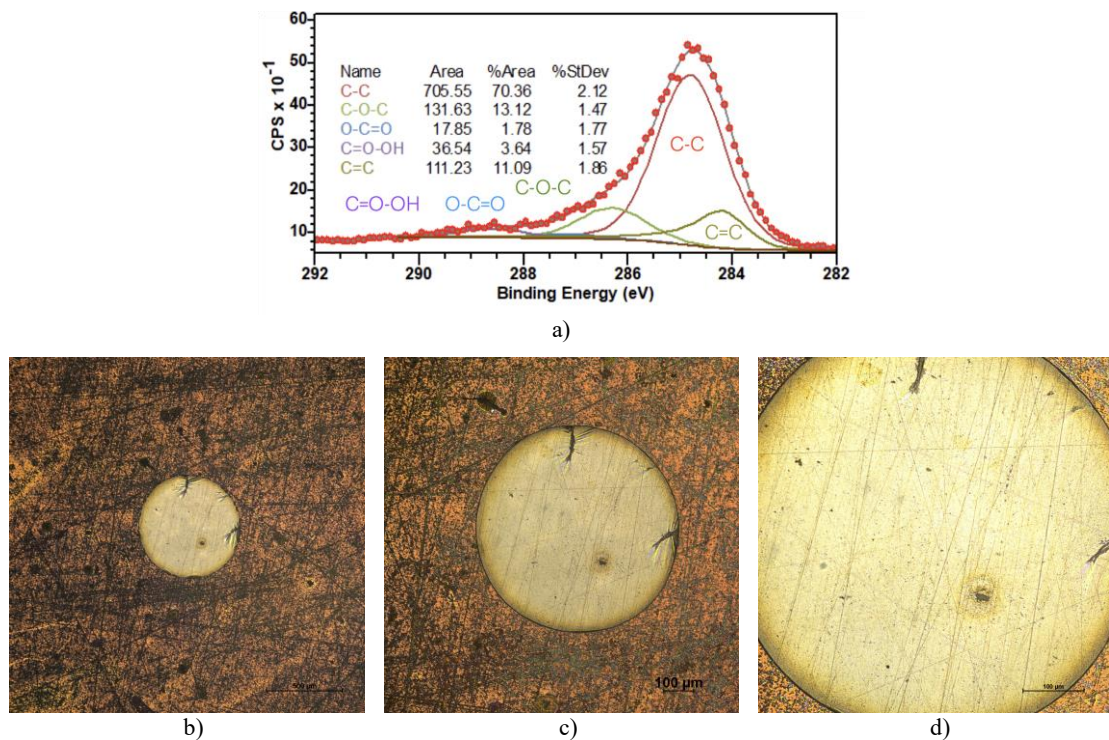


Fig. 5 – a) C 1s spectra for 53,6 nm DLC free-standing film and Optical Microscopy – (b), (c), (d).

Optical microscopy (Figs. 1–5, (b), (c), (d)) confirms the presence of continuous free-standing regions in all films. Observed thickness-dependent wrinkle patterns are consistent with standard stress-relief mechanisms in thin films and occur on length scales much larger than the laser focal spot. Consequently, these morphological features do not affect relativistic coupling, ensuring uniform interaction conditions across the target area.

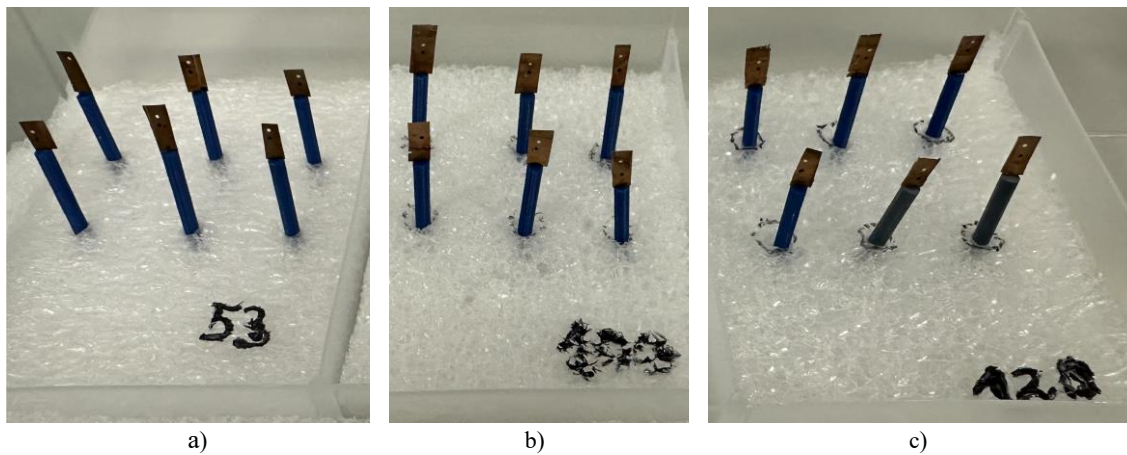


Fig. 6 – Example of a prepared batch of free-standing DLC targets with thicknesses of (a) 53 nm, (b) 100 nm, and (c) 120 nm, assembled and mounted for deployment in high-power laser experiments.

#### 4. CONCLUSIONS

PECVD-grown DLC films released through copper back-etching exhibit the structural integrity, chemical stability, and mechanical uniformity required for deployment as free-standing ultra-thin targets in petawatt-class laser–matter interaction experiments. Their high  $sp^3$  fractions, shallow and well-confined surface oxidation, and minimal residual contamination ensure predictable behaviour under extreme irradiation, consistent with performance trends reported in earlier DLC-based high-intensity studies [3, 4, 13, 15]. Optical microscopy confirms continuous, defect-free free-standing regions on the millimetre scale, with thickness-dependent wrinkling that remains irrelevant to relativistic laser coupling. Collectively, these results demonstrate that PECVD-grown DLC membranes provide a robust and reproducible target platform for advanced ion-acceleration investigations at facilities such as ELI-NP [1, 10].

Future developments will extend this capability through the fabrication of magnetron-sputtered DLC membranes released from NaCl sacrificial layers, a method previously demonstrated for accelerator-grade films [19, 20]. This complementary approach is expected to offer improved stress management, enhanced thickness uniformity, and expanded control over carbon hybridisation, thereby broadening the accessible parameter space for next-generation free-standing ultra-thin targets in relativistic laser–plasma experiments.

#### ACKNOWLEDGMENTS

The research was supported by the contract PN 23.21.01.06 sponsored by the Romanian Ministry of Research, Innovation, and Digitalisation.

#### REFERENCES

- [1] Dincă L, et al. Freestanding carbon targets for enhanced acceleration of carbon ions with petawatt-class lasers. U.P.B. Sci. Bull. Ser. A. 2023; 85(4): 171–178. [https://www.scientificbulletin.upb.ro/static/pdfs/rez1a1\\_218560.pdf](https://www.scientificbulletin.upb.ro/static/pdfs/rez1a1_218560.pdf)
- [2] Fernández JC, et al. Laser-plasmas in the relativistic-transparency regime: science and applications. Phys Plasmas. 2017; 24(5): 056702. <https://doi.org/10.1063/1.4983991>
- [3] Batignani G, Pontecorvo E, Giovannetti G, et al. Electronic resonances in broadband stimulated Raman spectroscopy. Sci Rep. 2016; 6: 18445. <https://doi.org/10.1038/srep18445>
- [4] Pan H, Chen B. Ultra-flexibility and unusual electronic, magnetic and chemical properties of waved graphenes and nanoribbons. Sci Rep. 2014; 4: 4198. <https://doi.org/10.1038/srep04198>
- [5] Henig A, et al. Radiation-pressure acceleration of ion beams driven by circularly polarized laser pulses. Phys Rev Lett. 2009; 103: 245003. <https://doi.org/10.1103/PhysRevLett.103.245003>
- [6] Fuchs J, et al. Laser-driven proton scaling laws and new paths towards energy increase. Nat Phys. 2006; 2(1): 48–54. <https://doi.org/10.1038/nphys199>

- [7] Macchi A, et al. Ion acceleration by superintense laser–plasma interaction. *Rev Mod Phys.* 2013; 85(2): 751–793. <https://doi.org/10.1103/RevModPhys.85.751>
- [8] Bachmann P, et al. Towards a general concept of diamond chemical vapour deposition. *Diam Relat Mater.* 1991; 1(1): 1–12. [https://doi.org/10.1016/0925-9635\(91\)90005-U](https://doi.org/10.1016/0925-9635(91)90005-U)
- [9] Nerat M, Černivec G, Smole F, Topič M. Simulation study of the effects of grain shape and size on the performance of Cu(In,Ga)Se<sub>2</sub> solar cells. *J Appl Phys.* 2008; 104(8): 083706. <https://doi.org/10.1063/1.2998908>
- [10] Dabu R. Femtosecond laser pulses amplification in crystals. *Crystals.* 2019; 9(7): 347. <https://doi.org/10.3390/cryst9070347>
- [11] Shin Y-M, Figora M. Instrumental development of a quasi-relativistic ultrashort electron beam source for electron diffractions and spectroscopies. *Rev Sci Instrum.* 2017; 88: 103302. <https://doi.org/10.1063/1.4994571>
- [12] Dollar F, et al. Scaling high-order harmonic generation from laser–solid interactions to ultrahigh intensity. *Phys Rev Lett.* 2013; 110: 175002. <https://doi.org/10.1103/PhysRevLett.110.175002>
- [13] Ma W, et al. Preparation of self-supporting diamond-like carbon nanofolios with thickness less than 5 nm for laser-driven ion acceleration. *Nucl Instrum Methods Phys Res B.* 2011; 655(1): 53–56. <https://doi.org/10.1016/j.nima.2011.06.019>
- [14] Kinoshita H, et al. Synthesis and mechanical properties of carbon nanotube/diamond-like carbon composite films. *Diam Relat Mater.* 2007; 16(11): 1940–1944. <https://doi.org/10.1016/j.diamond.2007.08.004>
- [15] Bin J, et al. Ion acceleration using relativistic pulse shaping in near-critical-density plasmas. *Phys Rev Lett.* 2015; 115: 064801. <https://doi.org/10.1103/PhysRevLett.115.064801>
- [16] Doumy G, et al. Complete characterization of a plasma mirror for the production of high-contrast ultraintense laser pulses. *Phys Rev E.* 2004; 69: 026402. <https://doi.org/10.1103/PhysRevE.69.026402>
- [17] Choi Y, et al. Reflection phase microscopy using spatio-temporal coherence of light. *Optica.* 2018; 5(11): 1468–1473. <https://doi.org/10.1364/OPTICA.5.001468>
- [18] Steinke S, et al. Efficient ion acceleration by collective laser-driven electron dynamics with ultra-thin foil targets. *Laser Part Beams.* 2010; 28: 215–221. <https://doi.org/10.1017/S0263034610000157>
- [19] Szerypo J, et al. Target fabrication for laser-ion acceleration research at the Technological Laboratory of the LMU Munich. *Matter Radiat Extremes.* 2019; 4: 035201. <https://doi.org/10.1063/1.5081807>
- [20] Liechtenstein V, et al. Preparation and evaluation of thin diamond-like carbon foils for heavy-ion tandem accelerators and time-of-flight spectrometers. *Nucl Instrum Methods Phys Res A.* 1997; 397: 140–145. [https://doi.org/10.1016/S0168-9002\(97\)00732-8](https://doi.org/10.1016/S0168-9002(97)00732-8)
- [21] Xiong X, et al. Manufacturing of free-standing diamond-like carbon (DLC) films for ultra-thin target applications. In: *Proc. 4th Int. Particle Accelerator Conf. (IPAC'13).* Shanghai, China; 2013 May. Geneva: JACoW Publishing; 2013.

*Received December 11, 2025*